Ca2+-dependent nuclear contraction in the heliozoon Actinophrys sol

Arikawa, Mikihiko ; Saito, Akira ; Omura, Gen ; Khan, S. M. Mostafa Kamal ; Suetomo, Yasutaka ; Kakuta, Soichiro ; Suzaki, Toshinobu

(Citation)
Cell Calcium,38(5):447-455

(Issue Date)
2005-11

(Resource Type)
journal article

(Version)
Accepted Manuscript

(URL)
https://hdl.handle.net/20.500.14094/90000975

Cell Calcium, Volume 38, Issue 5, November 2005, Pages 447-455.

Ca^{2+}-dependent nuclear contraction in the heliozoon *Actinophrys sol*

Mikihiko Arikawa[1, 2], Akira Saito[3], Gen Omura[2], S. M. Mostafa Kamal Khan[2], Yasutaka Suetomo[2], Soichiro Kakuta[2] and Toshinobu Suzaki[2]

[1]Department of Biological Sciences, Faculty of Science, Nara Women's University, Nara 630-8506, Japan

[2]Department of Biology, Faculty of Science, Kobe University, Kobe 657-8501, Japan

[3]Department of Histology and Cell Biology, Graduate School of Biomedical Science, Hiroshima University, Hiroshima 734-8551, Japan

Abbreviated title: Nuclear contraction in *Actinophrys sol*

Correspondence to: Mikihiko Arikawa, Department of Biological Sciences, Faculty of Science, Nara Women's University, Kitauoyanishi-machi, Nara 630-8506, Japan; Tel/Fax: +81-742-20-3421; e-mail: miki_arkw1974@ybb.ne.jp

Abstract

Ca^{2+}-dependent contractility was found to exist in the nucleus of the heliozoon protozoan *Actinophrys sol*. Upon addition of Ca^{2+} ($[Ca^{2+}]_{free} = 2.0 \times 10^{-3}$ M), diameters of isolated and detergent-extracted nuclei became reduced from 16.5 ± 1.7 μm to 11.0 ± 1.3 μm. The threshold level of $[Ca^{2+}]_{free}$ for the nuclear contraction was 2.9×10^{-7} M. The nuclear contraction was not induced by Mg^{2+}, and was not inhibited by colchicine or cytochalasin B. Contracted nuclei became expanded when Ca^{2+} was removed by EGTA; thus cycles of contraction and expansion could be repeated many times by alternating addition of Ca^{2+} and EGTA. The Ca^{2+}-dependent nuclear contractility remained even after high salt treatment, suggesting a possible involvement of nucleoskeletal components in the nuclear contraction. Electron microscopy showed that, in the relaxed state, filamentous structures were observed to spread in the nucleus to form a network. After addition of Ca^{2+}, they became aggregated and constructed a mass of thicker filaments, followed by re-distribution of the filaments spread around inside of the nucleus when Ca^{2+} was removed. These results suggest that the nuclear contraction is induced by Ca^{2+}-dependent transformation of the filamentous structures in the nucleus.

1. Introduction

A large number of investigations have been made on characteristic contractile systems in unicellular organisms. The spasmoneme of vorticellid ciliates [1-6], the myoneme of heterotrichous ciliates [7, 8], and the flagellar root of green algae [9-12] are well-known organelles which show Ca^{2+}-dependent contractility. Contraction of these organelles is considered to be generated by proteins such as centrin (caltractin) and spasmin [13, 14], which belong to the calmodulin subfamily. Although much progress has been made on characterization of such Ca^{2+}-binding proteins and resulting cytoplasmic contraction at a molecular level, less attention has so far been paid to the dynamics of the nucleus.

In 1974, a stable framework structure termed the "nuclear matrix" was found in an isolated rat liver nucleus by sequential chemical extractions [15, 16]. Since then, many investigations have been performed to elucidate possible functions of the nuclear matrix, and it is now clear that the nuclear matrix is involved in the processes of gene expression, replication and transcription of DNA, and also processing and transportation of RNA [17]. The ultrastructure of the nuclear matrix has also been well studied, and branched thin filaments with a diameter of about 10 nm were identified to construct the interior architecture of the nucleus [18]. Despite considerable advances in physiological and morphological investigations, evidence for the existence of contractility of the nuclear matrix has not been reported so far.

Recently, we reported that Ca^{2+}-dependent contractility exists in an isolated and demembranated macronucleus of the hypotrichous ciliate *Euplotes aediculatus* [19]. Furthermore, similar nuclear contraction was observed in several species of protozoan cells and even in cultured mammalian cells (HeLa cells). From these results, we have

proposed a hypothesis that all eukaryotic cells possess Ca^{2+}-dependent nuclear contractility which has been preserved during the process of eukaryotic evolution. As an example, isolated and detergent-extracted nuclei of the heliozoon *Actinophrys sol* were demonstrated to express the Ca^{2+}-dependent contractility. In the present study, physiological characterization of the contractility and ultrastructural observations of isolated nuclei were carried out, and a possible mechanism of the Ca^{2+}-dependent nuclear contraction is presented.

2. Materials and Methods

2.1. Organisms and culture

Actinophryid heliozoon *Actinophrys sol* (protozoa) was axenically cultured in a co-culturing condition with *Chlorogonium elongatum* in 10% artificial sea water (47 mM NaCl, 1.1 mM KCl, 1.1 mM $CaCl_2$, 2.5 mM $MgCl_2$, 2.5 mM $MgSO_4$ and 1 mM Tris-HCl, pH 7.8) containing 10% *Chlorogoniumu* medium (0.01% sodium acetate, 0.01% polypepton, 0.02% tryptone peptone, 0.02% yeast extract and 1 μg/ml $CaCl_2$) at 20 ± 1ºC under constant lighting. Subculturing was carried out at intervals of about 2 weeks. Centrifugally collected cells were gently washed with fresh 10% artificial sea water at room temperature before using for experiments.

2.2. Nuclear isolation procedures

Nuclei of *A. sol* were isolated by using a sucrose-Percoll separation technique. At first, a solution A consisting of 2.0 M sucrose, 10% Percoll, 3 mM ethylene glycol bis(β-aminoethylether)-N ,N ,N' ,N' –tetraacetic acid (EGTA) and 5 mM N-(2-Hydroxyethyl)piperazine-N'-2-ethanesulfonic acid (HEPES, pH 7.0) was overlaid in a test tube with a solution B consisting of 2.0 M sucrose, 3 mM EGTA and 5 mM HEPES (pH 7.0). Washed cells were centrifugally collected and suspended in a solution C consisting of 1.0 M sucrose, 3 mM EGTA and 5 mM HEPES (pH 7.0), homogenized with a Teflon homogenizer, and placed on top of the layered solutions in the test tube. To extract membraneous components from isolated nuclei, 1.0% Triton X-100 was added to the solution C. After centrifugation at 750 g for 10 min, isolated nuclei were collected from the boundary between solutions A and B. Nuclei were again suspended in solution C, and were centrifuged at 750 g for 5 min. After removal

of the supernatant, the crude preparation of the nuclear pellet was collected from the bottom of the test tube, and subjected to different concentrations of divalent cations for light microscopy or a fixative solution for electron microscopy.

2.3. Light microscopy

Isolated nuclei were placed on a glass slide coated with 0.1% poly-L-lysine. After covered with a coverslip, the nuclei were left for a few minutes until the nuclei became stuck to the glass surface. Test solutions were introduced from one side of the preparation using a Pasteur pipette, and were absorbed from the other side using a piece of filter paper. Although unattached nuclei were flushed away by a stream of test solutions, many nuclei remained on the substratum, which allowed us to observe nuclear responses continuously under an Olympus BX-50 microscope equipped with Nomarski differential interference optics. Images were recorded on a video cassette recorder (Victor, BR-S822) or a high resolution digital camera (Olympus DP11) for measurement of an approximate area of the isolated macronuclei using an image analyzing software Scion Image Beta 4.02 (Scion Corporation).

2.4. Electron microscopy

Isolated nuclei were prefixed with 3% glutaraldehyde in an EGTA buffer for 3 min at room temperature. They were then postfixed with a fixative consisting of 1% OsO_4, 0.01 mM $MgSO_4$, 1 mM sucrose, and 50 mM sodium cacodylate (pH 7.0) for 30 min at room temperature. After being washed with 50 mM cacodylate buffer (pH 7.0), fixed nuclei were dehydrated through a graded ethanol series, and embedded in Spurr's epoxy resin [20]. Thin sections were picked up on a Formver-coated copper grid, stained

with 3% aqueous uranyl acetate for 15 min and Reynolds' lead citrate [21] for 5 min at room temperature, and then observed under a transmission electron microscope (Hitachi H-7100) operated at 75 kV.

3. Results

3.1. Reduction in diameter of isolated nuclei

Actinophrys sol possesses a single nucleus within the cytoplasm. As shown in Fig. 1a, differential interference contrast light microscopy showed that the spherical nucleus (marked "N") was located at the center of the cell body, and cortical nucleolar materials were present at the inner periphery of the nucleus. In this study, Ca^{2+}-dependent contractility was found to exist in isolated and detergent-extracted nuclei. Although nucleolar material could no longer be observed after isolation, the spherical shape of the nucleus was well preserved (Fig. 1b). When nuclear isolation was performed in the presence of calcium ions (2×10^{-3} M free Ca^{2+}), the diameter of the nucleus decreased. Furthermore, the contour of the nucleus became prominent, and the nucleus showed a rigid appearance (Fig. 1c).

Diameters of isolated nuclei were measured under various conditions, and compared with those in living cells (Fig. 2). Nuclear diameters in living cells were in the range of 10.9 - 19.9 μm, with an average value of 15.1 ± 1.7 μm (Fig. 2a). In the absence of Ca^{2+}, average diameters of the nuclei isolated without (Fig. 2b) and with detergent treatment (Fig. 2d) were slightly larger (15.9 ± 1.5 μm and 16.5 ± 1.7 μm, respectively) than those in the living cells (Fig. 2a). On the contrary, average diameters of nuclei isolated without (Fig. 2c) and with detergent treatment (Fig. 2e) in a Ca^{2+}-containing solution (2×10^{-3} M free Ca^{2+}) were significantly smaller (12.4 ± 1.1

μm and 11.0 ± 1.3 μm, respectively). Compared with the nuclei in living cells, as shown in Fig. 2f, no significant differences in the nuclear diameter were observed when nuclei were isolated in a solution containing 2 mM free Mg^{2+} (14.8 ± 1.4 μm on average). These results show that the diameters of isolated nuclei were decreased in a Ca^{2+}-dependent manner. The diameter reduction of the isolated nucleus was observed even in the presence of colchicine (10 mM) and cytochalasin B (1 mM), suggesting that the mechanism of nuclear contraction may differ from that of actin-myosin and tubulin-dynein interactions.

Diameters of isolated nuclei (n = 140) were measured individually before and after induction of Ca^{2+}-dependent nuclear contraction (Fig. 3a). When the nuclear contraction occurs, the diameter of relaxed nuclei that ranged from 13.1 to 23.7 μm (17.8 ± 2.6 μm on average) decreased to 12.7 ± 1.9 μm on average with the range from 8.9 to 17.3 μm. The correlation coefficient between diameters of relaxed and contracted nucleus was calculated to be 0.74, which indicates that the degree of contraction is not significantly correlated with the nuclear size. The degree of nuclear contraction calculated from the average diameters measured before and after contraction was 63.7%. As shown in Fig. 3b, the degree of contraction was estimated and plotted against the volume of the relaxed nucleus. More than 80% of the nuclei showed 50 - 80% contraction, although a few small nuclei (< 4,000 μm^3 in volume) showed less contractility (20 - 30%).

3.2. Ca^{2+}-dependency of the nuclear contraction

As described in the “Materials and Methods”, isolated nuclei were attached to a glass surface and the Ca^{2+} influence on nuclear morphology was continuously observed

under a light microscope. The contraction and expansion cycle of an isolated and adhered nucleus could be repeated many times by alternating addition of Ca^{2+} and EGTA (Fig. 4), which indicates that such cycles were mediated by Ca^{2+} only without any other energy supply. Nuclei isolated in an EGTA solution were in a state of relaxation. They contracted on addition of Ca^{2+} (2×10^{-3} M Ca^{2+}, open arrowheads), and expanded upon subsequent addition of EGTA (filled arrowheads). Both contraction and expansion occurred within a few seconds after addition of Ca^{2+} and EGTA, respectively.

An isolated nucleus was attached to a glass surface and was treated with various concentrations of Ca^{2+}. The fractional volume of a responding nucleus was measured during both contraction and expansion processes and shown in Fig. 5. In the contraction process (open circles), the nucleus isolated in an EGTA solution became slightly contracted when 1×10^{-7} M Ca^{2+} was added, and it contracted completely when Ca^{2+} concentration was increased ($> 10^{-6}$ M). The degree of contraction of the fully-contracted nucleus reached around 60%. During the process of expansion (filled circles), the contracted nucleus recovered almost to its initial shape when Ca^{2+} concentration was lowered ($< 10^{-7}$ M). After full expansion, although the reason remains unclear, the volume of the nucleus tended to become larger than that of the nucleus before contraction. Ca^{2+} thresholds, or half-maximum concentrations of Ca^{2+}, for contraction and expansion of the nucleus were estimated by fitting the data with sigmoidal curves to be 2.9×10^{-7} M and 1.0×10^{-7} M, respectively.

3.3. Change of the image profile at nuclear contraction

To obtain high contrast images, we used a light microscope (Olympus BX-50)

equipped with Nomarski differential interference contrast (DIC) optics and a high resolution digital camera (Olympus DP11). As shown in the inserted light micrograph in Fig. 6a, the surface of an isolated nucleus appeared smooth, and no structural components were observed inside the nucleus. Using DIC optics, the left-side of the nuclear edge appeared as a bright crescent, while the opposite side appeared as a dark crescent. The DIC effect on the nucleus was also represented as image intensity profiles (Figs. 6a and b), in which the image intensities in the rectangles were analyzed. In the case of a relaxed nucleus in EGTA solution (Fig. 6a), a peak of brightness (open arrow) is present that represents the location of the left-side edge of the nucleus. The brightness profile has a depression at the right edge of the nucleus as shown by a filled arrow. The intensity profile inside the nucleus shows a smooth curve. These characteristics indicate that the optical density in the nucleus is different from the surrounding medium, and that the nucleus is composed of an optically uniform material. When the isolated nucleus became contracted on addition of Ca^{2+}, the appearance of the nucleus and its brightness profile changed markably, as shown in Fig. 6b. Nuclear diameter was reduced from 20 to 13 μm. Brightness increased at the left edge of the nucleus (open arrow), while it decreased at the right edge (filled arrow). The change was accompanied by a decrease and an increase of the brightness at regions just beneath the left and right edges as shown in the figure by filled and open arrowheads, respectively. Furthermore, brightness inside the nucleus became rough and irregular. Such changes in appearances and brightness pattern suggest that optical density inside the nucleus increased, especially in the periphery of the nucleus, when contraction occurred.

3.4. Ultrastructural observations

In this study, electron microscopy was carried out to examine ultrastructural changes inside nuclei that might have happened during nuclear contraction in responses to the addition of Ca^{2+}. As shown in Fig. 7a, in the nucleus in a living cell, a large amount of electron dense nucleolar material was located just beneath the inner surface of the nuclear envelope, and thin filaments were scattered to form a meshwork inside the nucleus. Although the nucleolar material disappeared during nuclear isolation, the spherical shape of the isolated nucleus was preserved (Fig. 7b1). In an enlarged micrograph, the dispersed meshwork of thin filaments was also well preserved (Fig. 7b2). When Ca^{2+} (2 mM) was added to the isolated and detergent-extracted nucleus, the thin filaments became aggregated and dramatically changed their appearance to a mass of thicker filaments (Fig. 7c). After the Ca^{2+}-induced aggregation of the thin filaments occurred, the nucleoplasm other than the thick filaments appeared sparse, while the inner layer of the nuclear membrane became dense comparatively in appearance. On subsequent addition of EGTA to the nucleus, these thick filaments became disintegrated and loose, resulting in re-distribution of the thin filament dispersed around the inside of the nucleus (Fig. 7d).

4. Discussion

In this study, we investigated Ca^{2+}-dependent contractility of isolated and detergent-extracted nuclei of the heliozoon *Actinophrys sol*. In actinophryid heliozoons such as *Actinophrys* and *Echinosphaerium*, cytoplasmic contraction is commonly observed during the process of food uptake. Heliozoon cells possess a large number of needle-like axopodia that radiate from their spherical cell bodies. When a small organism comes into close contact with the surface of an axopodium, rapid shortening of the axopodium occurs, and an attached prey organism is conveyed toward the cell body [22-24]. Inside the axopodium, a bundle of cytoskeletal microtubules extends along the length of the axopodium [25-28]. A bundle of contractile filamentous structures termed "contractile tubules structure (CTS)" also runs parallel to the axopodial microtubules [23, 29]. Electron microscopy has shown that the CTS changes its appearance from tubular to granular forms inside a contracted cytoplasm when the axopodial contraction occurs [30-34]. By using permeabilized cell models, it has been found that the driving force for axopodial contraction is not generated by disassembly of the axonemal microtubules, and that Ca^{2+}-dependent transformation of the CTS is responsible for the motility [35-37]. In this study, isolated and detergent-extracted nuclei showed Ca^{2+}-dependent contractility similar to that of the cytoplasm of permeabilized cell models. When cytoplasmic contraction of the permeabilized cell model was induced by an addition of Ca^{2+}, simultaneous contraction of the nuclei was also observed [36]. Detailed ultrastructural observations of the nucleus throughout the stages of the vegetative life cycle of *A. sol* have shown that the CTS is not present in the nucleus [38, 39]. Therefore, it is not possible to explain the mechanism of nuclear contraction by transformation of the CTS. Although

the CTS is present near the periphery of the nucleus where axonemal microtubules terminate [23], it seems unlikely that the CTS is also associated with the outer surface of the nucleus and regulates nuclear contraction. Judging from the electron microscopic observation that no CTS was present on the outer surface of isolated nuclei, the driving force responsible for the nuclear contraction may be generated inside the nucleus.

Isolated *Tetrahymena* macronuclei were reported in 1977 to show Ca^{2+}-dependent reversible contraction by a mechanism differing from the actin-myosin contraction system [40]. By counting the frequency of nuclear pore complexes per unit area in both contracted and expanded macronuclei, the contraction was attributed to contraction of the nuclear membrane [41]. Moreover, atomic force microscopy has revealed that the nuclear contraction can be explained by a calcium-sensitive shape change of individual nuclear pore complexes [42-44]. However, in the present study, nuclear membranes and intact nuclear pore complexes are unlikely to be preserved in the isolated and detergent-extracted nuclei of *A. sol*. In the isolated macronucleus of *Euplotes*, Ca^{2+}-dependent contraction was also observed even after the macronucleus had been completely demembranated [19, 45]. These facts indicate that neither nuclear membranes nor nuclear pore complexes are involved in the nuclear contraction.

As shown in Fig. 4, contraction and expansion of an adhered nucleus were completed within a few seconds. It might be possible to explain the dynamics of the isolated nucleus by the mechanism of de- and re-polymerization of certain filamentous structures such as F-actin and microtubules. For example, the speed of rapid disassembly of axonemal microtubules in heliozoon *Raphidiophrys contractilis* was estimated to be more than 3.0 mm/sec [46]. Furthermore, actin, myosin, and tubulin

molecules have been detected in the nuclei of various kinds of cells [47-50]. However, no direct evidence has been reported so far that these molecules are involved in nuclear contraction. In this study, contraction and expansion of the adhered nuclei were observed in a Ca^{2+}-dependent manner without any other energy supply, and were able to be repeatedly induced even in the presence of colchicine (10 mM) and cytochalasin B (1 mM), indicating that the mechanism of the nuclear contraction in *A. sol* may differ from microtubule- or actomyosin-based machineries. The contraction-expansion cycle of isolated nuclei was observed even after high salt treatment with 2 M NaCl for 30 min (data not shown), which suggests a possible involvement of the nucleoskeletal components in the Ca^{2+}-dependent nuclear contraction.

The nuclear matrix is defined as a residual nuclear framework obtained after sequential extraction procedures, and consists of two components: the nuclear lamina and an internal nuclear network [18, 51]. The inner nuclear architecture is connected to the nuclear lamina and built on an underlying network of branched 10 nm filaments [52, 53]. It is widely understood that nuclear lamins are major constituent proteins of the nuclear lamina which constructs a mesh-like network of intermediate filaments underlying the inner periphery of the nuclear membrane [54-56]. Recent studies have revealed that the lamins are present not only at the periphery of the nucleus but also within the nucleoplasm, and form an internal nucleoskeleton as well as a peripheral lamina [57-61]. It may be natural to consider that the network structure inside the nucleus in *A. sol* may also be constructed by 10 nm intermediate filaments or lamina because it is now widely believed that the nuclear matrix is a ubiquitous nuclear structure in all eukaryotic cells. Although, unfortunately, we could not detect nuclear lamin proteins by using a commercially-available anti-lamin antibody, the fact that the

nuclear matrix has been detected in nuclei of various unicellular organisms such as *Tetrahymena* [40, 62], *Amphidinium* [63] and *Euglena* [64] strongly suggests that the meshwork structure observed inside the isolated and detergent-extracted nucleus of *A. sol* is a nuclear matrix constructed by the nuclear lamina. Thus, our observations also support the idea that the nuclear matrix structure has been highly conserved during the eukaryotic evolution. However, there is no molecular clue to explain the Ca^{2+}-dependent contractility of the nuclear matrix. Our findings reported in this study suggest the possibility for the first time that the nucleus possesses contractility which is regulated by Ca^{2+}-dependent dis- and re-aggregation of the nuclear lamina filaments.

An alternative possibility is that the nuclear contraction is directly or indirectly mediated by a certain Ca^{2+}-binding protein. A large number of studies have revealed that Ca^{2+}-binding proteins exist within various kinds of nuclei, and play important roles in many nuclear events [65-69]. However, Ca^{2+}-dependent functions of these proteins are not entirely clear. In spite of an attempt to detect Ca^{2+}-binding proteins in this study by using "Stains-all" and "ruthenium red" staining methods or a Ca^{2+}-dependent mobility shift assay on separated nuclear proteins by SDS-PAGE, we could not obtain any positive results. Further physiological and morphological studies might allow us to understand the molecular mechanism, the intracellular functions, and biological significance of the Ca^{2+}-dependent nuclear contraction.

Acknowledgements

We are grateful to Dr. Adrienne Hardham for her critical reading of the manuscript. This work was partly supported by a Research Fellowship of the Japan Society for the Promotion of Science (JSPS) for Young Scientists to MA, and by the River

Environment Fund (REF) in charge of the Foundation of River and Watershed Environment Management (FOREM) to TS.

References

[1] H. Asai, T. Ochiai, K. Fukui, M. Watanabe, F. Kano, Improved preparation and cooperative calcium contraction of glycerinated *Vorticella*, J Biochem. 83 (1978) 795-798.

[2] T. Ochiai, H. Asai, K. Fukui, Hysteresis of contraction-extension cycle of glycerinated *Vorticella*, J Protozool. 26 (1979) 420-425.

[3] Y. Yokoyama, H. Asai, Contractility of the spasmoneme in glycerinated *Vorticella* stalk induced by various divalent metal and lanthanide ions, Cell Motil Cytoskel. 7 (1987) 39-45.

[4] K. Katoh, Y. Naitoh, Control of cellular contraction by calcium in *Vorticella*, J Exp Biol. 189 (1994) 163-177.

[5] K. Katoh, M. Kikuyama, An all-or-nothing rise in cytosolic [Ca^{2+}] in *Vorticella* sp, J Exp Biol. 200 (1997) 35-40.

[6] Y. Moriyama, S. Hiyama, H. Asai, High-speed video cinematographic demonstration of stalk and zooid contraction of *Vorticella convallaria*, Biophys J. 74 (1998) 487-491.

[7] H. Ishida, Y. Shigenaka, Cell model contraction in the ciliate *Spirostomum*, Cell Motil Cytoskel. 9 (1988) 278-282.

[8] H. Ishida, T. Suzaki, Y. Shigenaka, Effect of Mg^{2+} on Ca^{2+}-dependent contraction of a *Spirostomum* cell model, Europ J Protistol. 32 (1996) 316-319.

[9] J.L. Salisbury, G.L. Floyd, Calcium-induced contraction of the rhizoplast of a quadriflagellate green alga, Science. 202 (1978) 975-977.

[10] J.L. Salisbury, A. Baron, B. Surek, M. Melkonian, Striated flagellar roots: isolation and partial characterization of a calcium-modulated contractile organelle, J Cell

Biol. 99 (1984) 962-970.

[11] D.E. Coling, J.L. Salisbury, Characterization of the calcium-binding contractile protein centrin from *Tetraselmis striata* (Pleurastrophyceae), J Protozool. 39 (1992) 385-391.

[12] J.L. Salisbury, Roots, J Eukaryot Microbiol. 45 (1998) 28-32.

[13] C. David, B. Viguès, Calmyonemin: A 23 kDa analogue of algal centrin occurring in contractile myonemes of *Eudiplodinium maggii* (Ciliate), Cell Motil Cytoskel. 27 (1994) 169-179.

[14] J.J. Maciejewski, E.J. Vacchiano, S.M. Mccutcheon, H.E. Buhse Jr, Cloning and expression of a cDNA encoding a *Vorticella convallaria* spasmin: an EF-hand calcium-binding protein, J Eukaryot Microbiol. 46 (1999) 165-173.

[15] R. Berezney, D.S. Coffey, Identification of a nuclear protein matrix, Biochem Biophys Res Commun. 60 (1974) 1410-1417.

[16] R. Berezney, D.S. Coffey, Nuclear matrix. Isolation and characterization of a framework structure from rat liver nuclei, J Cell Biol. 73 (1977) 616-637.

[17] T. Pederson, Thinking about a nuclear matrix, J Mol Biol. 277 (1998) 147-159.

[18] J.A. Nickerson, Experimental observations of a nuclear matrix, J Cell Sci. 114 (2001) 463-474.

[19] M. Arikawa, N. Momokawa, A. Saito, G. Omura, S.M.M.K. Khan, Y. Suetomo, S. Kakuta, T. Suzaki, Ca^{2+}-dependent contractility of isolated and demembranated macronuclei in the hypotrichous ciliate *Euplotes aediculatus*, Cell Calcium. 33 (2002) 113-117.

[20] A.R. Spurr, A low-viscosity epoxy resin embedding medium for electron microscopy, J Ultrastruct Res. 26 (1969) 31-43.

[21] E.S. Reynolds, The use of lead citrate at high pH as an electron-opaque stain in electron microscopy, J Cell Biol. 17 (1963) 208-211.

[22] C.D. Ockleford, J.B. Tucker, Growth, breakdown, repair, and rapid contraction of microtubular axopodia in the heliozoan *Actinophrys sol*, J Ultrastruct Res. 44 (1973) 369-387.

[23] T. Suzaki, Y. Shigenaka, S. Watanabe, A. Toyohara, Food capture and ingestion in the large heliozoan, *Echinosphaerium nucleofilum*, J Cell Sci. 42 (1980) 61-79.

[24] M. Sakaguchi, K. Hausmann, T. Suzaki, Food capture and adhesion by the heliozoon *Actinophrys sol*, Protoplasma. 203 (1998) 130-137.

[25] L.G. Tilney, K.R. Porter, Studies on microtubules in heliozoa. I. The fine structure of *Actinosphaerium nucleofilum* (Barrett), with particular reference to the axial rod structure, Protoplasma. 60 (1965) 317-344.

[26] L.G. Tilney, Y. Hiramoto, D. Marsland, Studies on the microtubules in heliozoa. III. A pressure analysis of the role of these structures in the formation and maintenance of the axopodia of *Actinosphaerium nucleofilum* (Barrett), J Cell Biol. 29 (1966) 77-95.

[27] C.D. Ockleford, Cytokinesis in the heliozoan *Actinophrys sol*, J Cell Sci. 16 (1974) 499-517.

[28] Y. Shigenaka, M. Kaneda, Studies on the cell fusion of heliozoans. IV. An electron microscopical study on the fusion process accompanied with axopodial degradation, Annot Zool Japon. 52 (1979) 28-39.

[29] Y. Shigenaka, K. Yano, R. Yogosawa, T. Suzaki, Rapid contraction of the microtubules-containing axopodia in a large heliozoan *Echinosphaerium*, In: H. Sakai, H. Mohri, G.G. Borisy (Ed.), Biological functions of microtubules and

related structures, Tokyo, Japan, Academic Press, 1982: pp. 105-114.

[30] T. Matsuoka, Y. Shigenaka, Y. Naitoh, A model of contractile tubules showing how they contract in the heliozoan *Echinosphaerium*, Cell Struct Funct. 10 (1985) 63-70.

[31] M. Ando, Y. Shigenaka, Structure and function of the cytoskeleton in heliozoa. I. Mechanism of rapid axopodial contraction in *Echinosphaerium*, Cell Motil Cytoskel. 14 (1989) 288-301.

[32] M. Sugiyama, S. Ikegawa, E. Masuyama, T. Suzaki, M. Ishida, Y. Shigenaka, Isolation and properties of the axopodial cytoskeleton of a heliozoan, *Echinosphaerium akamae*, Europ J Protistol. 28 (1992) 214-219.

[33] T. Suzaki, M. Ando, Y. Inai, Y. Shigenaka, Structure and function of the cytoskeleton in heliozoa. III. Rapid microtubule disorganization during axopodial contraction in *Echinosphaerium*, Europ J Protistol. 30 (1994) 404-413.

[34] E. Kinoshita, Y. Shigenaka, T. Suzaki, The ultrastructure of contractile tubules in the heliozoon *Actinophrys sol* and their possible involvement in rapid axopodial contraction, J Eukaryot Microbiol. 48 (2001) 519-526.

[35] T. Suzaki, M. Ando, K. Ishigame, Y. Shigenaka, M. Sugiyama, Structure and function of the cytoskeleton in heliozoa. II. Measurement of the force of rapid axopodial contraction in *Echinosphaerium*, Europ J Protistol. 28 (1992) 430-433.

[36] M. Arikawa, T. Suzaki, Reactivation of Ca^{2+}-dependent cytoplasmic contraction in permeabilized cell models of the heliozoon *Echinosphaerium akamae*, Cell Motil Cytoskel. 53 (2002) 267-272.

[37] M. Arikawa, A. Saito, G. Omura, S.M.M.K. Khan, E. Kinoshita, T. Suzaki, Ca^{2+}-dependent cytoplasmic contractility of the heliozoon *Actinophrys sol*, Europ J

Protistol. 38 (2002) 365-372.

[38] J.P. Mignot, Étude ultrastructurale de la pédogamie chez *Actinophrys sol* (heliozoaire). II. Les divisions de maturation, Protistologica T. XVI (1980) 205-225.

[39] J.P. Mignot, Étude ultrastructurale de la mitose végétative chez l'héliozoaire *Actinophrys sol*, Protistologica T. XX (1984) 247-263.

[40] F. Wunderlich, G. Herlan, A reversibly contractile nuclear matrix. Its isolation, structure, and composition, J Cell Biol. 73 (1977) 271-278.

[41] F. Wunderlich, G. Giese, C. Bucherer, Expansion and apparent fluidity decrease of nuclear membranes induced by low Ca/Mg. Modulation of nuclear membrane lipid fluidity by the membrane-associated nuclear matrix proteins? J Cell Biol. 79 (1978) 479-490.

[42] A. Rakowska, T. Danker, S.W. Schneider, H. Oberleithner, ATP-induced shape change of nuclear pores visualized with the atomic force microscope, J Membr Biol. 163 (1998) 129-136.

[43] H. Oberleithner, Aldosterone and nuclear signaling in kidney, Steroids. 64 (1999) 42-50.

[44] T. Danker, H. Oberleithner, Nuclear pore function viewed with atomic force microscopy, Eur J Physiol. 439 (2000) 671-681.

[45] M. Arikawa, A. Watanabe, K. Watanabe, T. Suzaki, High-resolution scanning electron microscopy of chromatin bodies and replication bands of isolated macronuclei in the hypotrichous ciliate *Euplotes aediculatus*, Europ J Protistol. 36 (2000) 40-45.

[46] S.M.M.K. Khan, M. Arikawa, G. Omura, Y. Suetomo, S. Kakuta, T. Suzaki,

Axopodial contraction in the heliozoon *Raphidiophrys contractilis* requires extracellular Ca^{2+}, Zool Sci. 20 (2003) 1367-1372.

[47] A.S. Douvas, C.A. Harrington, J. Bonner, Major nonhistone proteins of rat liver chromatin: preliminary identification of myosin, actin, tubulin, and tropomyosin (contractile proteins/ endogenous protease digestion of chromatin), Proc Natl Acad Sci USA. 72 (1975) 3902-3906.

[48] M. Berrios, P.A. Fisher, A myosin heavy chain-like polypeptide is associated with the nuclear envelope in higher eukaryotic cells, J Cell Biol. 103 (1986) 711-724.

[49] M. Berrios, P.A. Fisher, E.C. Matz, Localization of a myosin heavy chain-like polypeptide to *Drosophila* nuclear pore complexes, Proc Natl Acad Sci USA. 88 (1991) 219-223.

[50] G. Nowak, L. Pestic-Dragovich, P. Hozák, A. Philimonenko, C. Simerly, G. Schatten, P. de Lanerolle, Evidence for the presence of myosin I in the nucleus, J Biol Chem. 272 (1997) 17176-17181.

[51] A.M. Martelli, E. Falcieri, M. Zweyer, R. Bortul, G. Tabellini, A. Cappellini, L. Cocco, L. Manzoli, The controversial nuclear matrix: a balanced point of view, Histol Histopathol. 17 (2002) 1193-1205.

[52] D. He, J.A. Nickerson, S. Penman, Core filaments of the nuclear matrix, J Cell Biol. 110 (1990) 569-580.

[53] J.A. Nickerson, G. Krockmalnic, K.M. Wan, S. Penman, The nuclear matrix revealed by eluting chromatin from a cross-linked nucleus, Proc Natl Acad Sci USA. 94 (1997) 4446-4450.

[54] U. Aebi, J. Cohn, L. Buhle, L. Gerace, The nuclear lamina is a meshwork of intermediate-type filaments, Nature. 323 (1986) 560-564.

[55] E.A. Nigg, Assembly-disassembly of the nuclear lamina, Curr Opin Cell Biol. 4 (1992) 105-109.

[56] R.D. Moir, R.D. Gorldman, Lamin dynamics, Curr Opin Cell Biol. 5 (1993) 408-411.

[57] A.S. Belmont, Y. Zhai, A. Thilenius, Lamin B distribution and association with peripheral chromatin revealed by optical sectioning and electron microscopy tomography, J Cell Biol. 123 (1993) 1671-1685.

[58] J.M. Bridger, I.R. Kill, M. O'Farrell, C.J. Hutchison, Internal lamin structures within G_1 nuclei of human dermal fibroblasts, J Cell Sci. 104 (1993) 297-306.

[59] R.D. Moir, M. Michelle-Lowy, R.D. Goldman, Dynamic properties of nuclear lamins: Lamin B is associated with sites of DNA replication, J Cell Biol. 125 (1994) 1201-1212.

[60] P. Hozák, A.M. Sasseville, Y. Raymond, P.R. Cook, Lamin proteins form an internal nucleoskeleton as well as a peripheral lamina in human cells, J Cell Sci. 108 (1995) 635-644.

[61] L.M. Neri, Y. Raymond, A. Giordano, S. Capitani, A.M. Martelli, Lamin A is part of the internal nucleoskeleton of human erythroleukemia cells, J Cell Physiol. 178 (1999) 284-295.

[62] G. Herlan, F. Wunderlich, Isolation of a nuclear protein matrix from Tetrahymena macronuclei, Cytobiologie. 13 (1976) 291-296.

[63] A. Mínguez, S. Franca, S. Moreno Díaz de la Espina, Dinoflagellates have a eukaryotic nuclear matrix with lamin-like proteins and topoisomerase II, J Cell Sci. 107 (1994) 2861-2873.

[64] J. Wen, The nuclear matrix of *Euglena gracilis* (Euglenophyta): A stage of nuclear

matrix evolution? Biol Cell. 92 (2000) 125-131.

[65] J.S.C. Gilchrist, G.N. Pierce, Identification and purification of a calcium-binding protein in hepatic nuclear membranes, J Biol Chem. 268 (1993) 4291-4299.

[66] J.S.C. Gilchrist, M.P. Czubryt, G.N. Pierce, Calcium and calcium-binding proteins in the nucleus, Mol Cell Biochem. 135 (1994) 79-88.

[67] M.P. Czubryt, B. Ramjiawan, J.S.C. Gilchrist, H. Massaeli, G.N. Pierce, The presence and partitioning of calcium binding proteins in hepatic and cardiac nuclei, J Mol Cell Cardiol. 28 (1996) 455-465.

[68] M.N. Badminton, J.M. Kendall, C.M. Rembold, A.K. Campbell, Current evidence suggests independent regulation of nuclear calcium, Cell Calcium. 23 (1998) 79-86.

[69] J.S.C. Gilchrist, B. Abrenica, P.J. DiMario, M.P. Czubryt, G.N. Pierce, Nucleolin is a calcium-binding protein, J Cell Biochem. 85 (2002) 268-278.

Figure legends

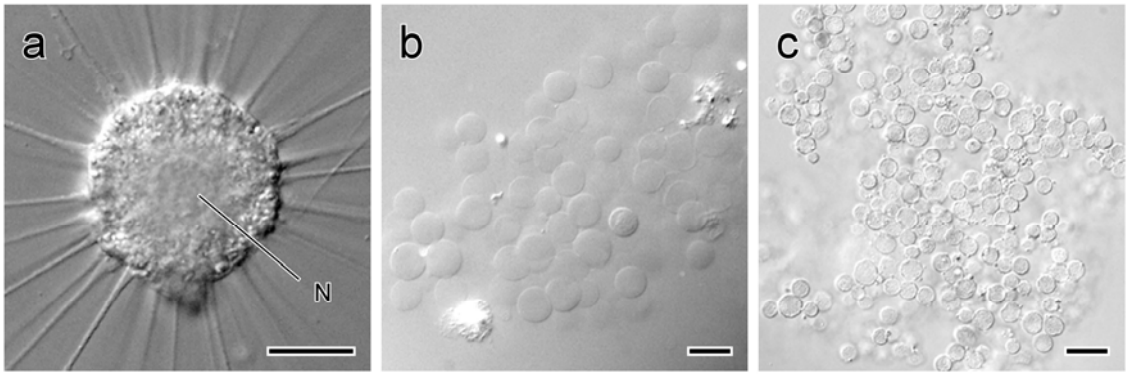

Fig. 1. Light micrographs of *Actinophrys sol*. (a) A living cell possesses a single spherical nucleus (N) at the center of the cell body. (b) Isolated nuclei in a Ca^{2+}-free solution. The spherical shape of the nucleus was well preserved after isolation and detergent-extraction with 1.0% Triton X-100. (c) When nuclei were isolated in a Ca^{2+}-containing solution (2 mM free Ca^{2+}), diameters of the nuclei became reduced and the periphery of the nuclei showed sharp profiles. Bars = 20 μm.

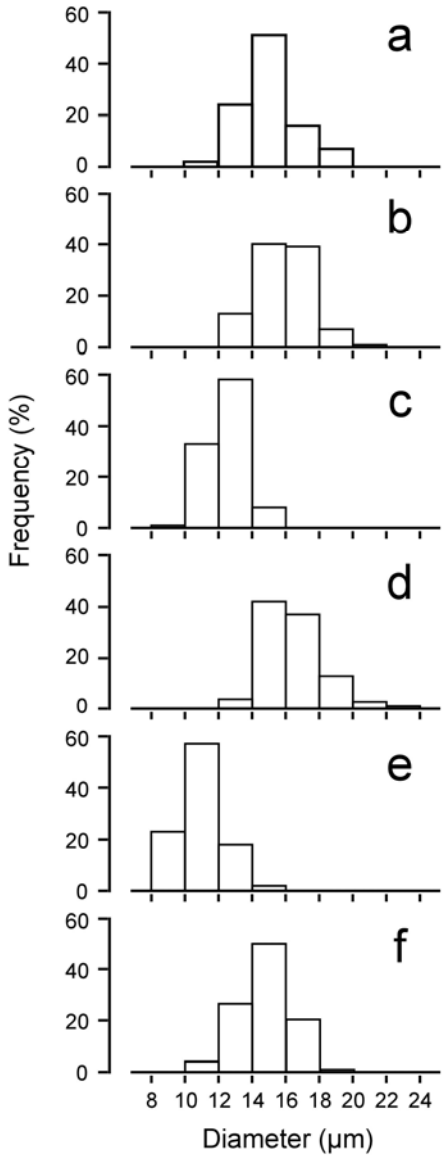

Fig. 2. Ca^{2+}-dependent diameter reduction of isolated nuclei. a, nuclei observed in living cells. b - f, isolated nuclei. Compared with the living cells (a), no diameter reduction was observed in nuclei isolated in Ca^{2+}-free solutions by either homogenization (b) or detergent treatment (d). When nuclei were isolated in Ca^{2+}-containing solutions (2 mM free Ca^{2+}) by homogenization (c) or detergent treatment (e), diameter reduction was significantly observed. Mg^{2+} (2 mM) did not induce the reduction of nuclear diameter (f).

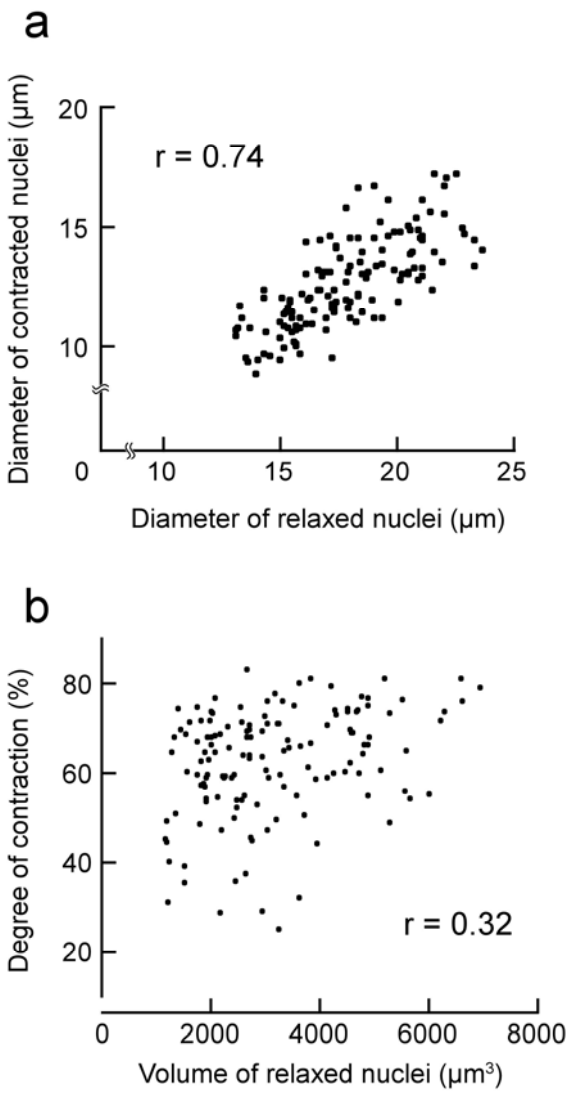

Fig. 3. (a) Relationship between diameters of isolated nuclei (n = 140) measured before and after contraction. On the addition of Ca^{2+} (2 mM), diameters of relaxed nuclei ranging from 13.1 to 23.7 μm decreased to a value between 8.9 and 17.3 μm. The correlation coefficient between diameters of relaxed and contracted nucleus was calculated to be 0.74. (b) Relationship between the degree of nuclear contraction and the volume of relaxed nuclei. The degree of contraction (D) was calculated as: D = 100 - 100 × (Vco / Vre), where Vre and Vco are the volume of the relaxed and contracted nucleus, respectively. More than 80% of nuclei showed 50 to 80%

contraction.

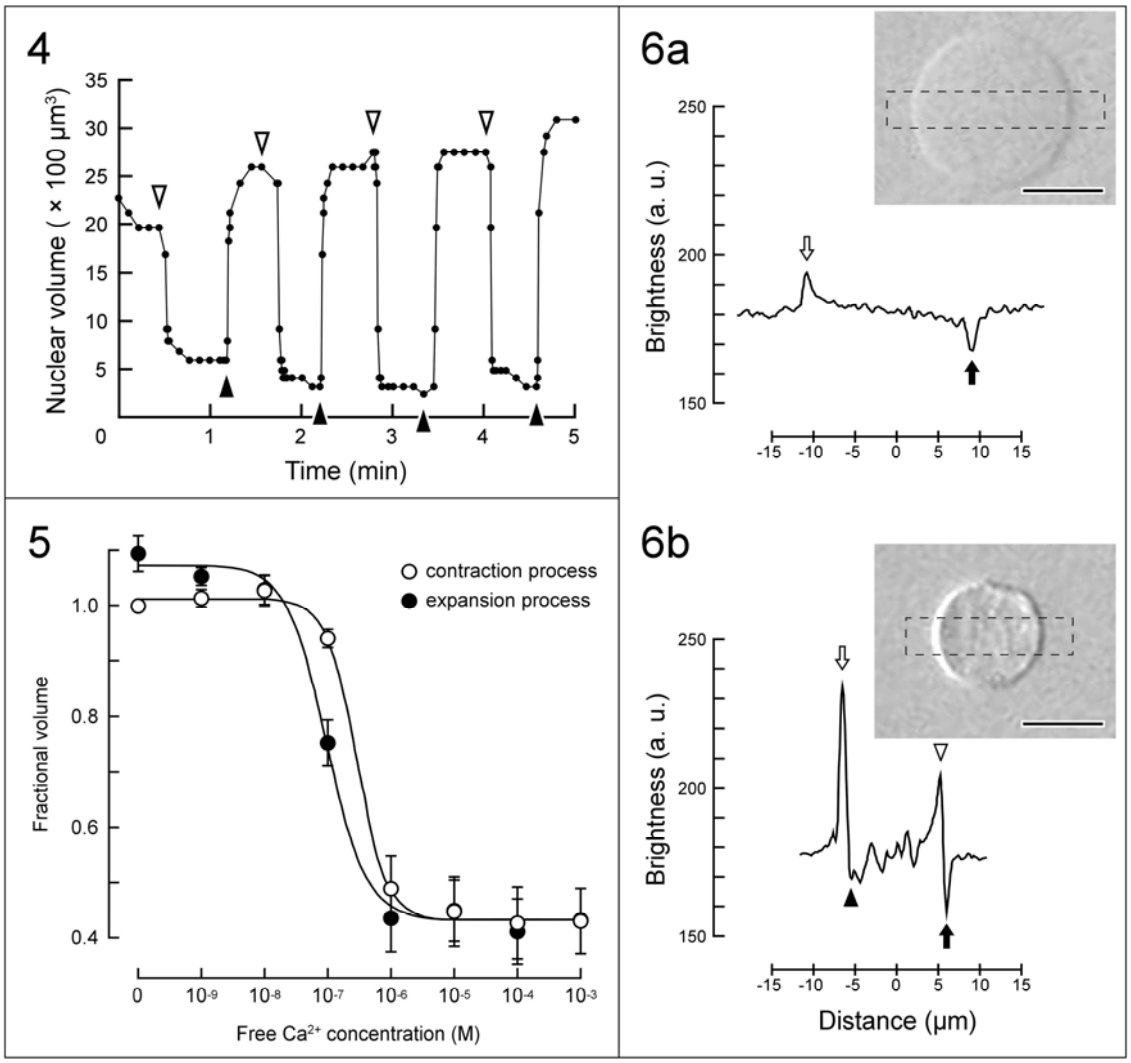

Fig. 4. Sequential measurement of the nuclear volume during cyclic contraction and expansion. An isolated nucleus contracted on addition of 2 mM Ca^{2+} (open arrowheads), and re-expanded upon subsequent addition of EGTA (filled arrowheads). Such cycles could be repeated many times by alternating addition of Ca^{2+} and EGTA.

Fig. 5. Ca^{2+}-dependent contraction and expansion of isolated nuclei. When Ca^{2+} concentration was raised stepwise, an isolated nucleus contracted with the threshold Ca^{2+} level of 2.9×10^{-7} M, and reached up to around 60% of contraction. The contracted nucleus expanded gradually when Ca^{2+} concentration was lowered, and the

threshold level of Ca^{2+} for the nuclear expansion was 1.0×10^{-7} M. Open and filled circles represent the processes of contraction and expansion, respectively.

Fig. 6. Changes in brightness profiles of an isolated nucleus during contraction. Vertical and lateral axes of the graphs represent averaged brightness in the delimited area (rectangles with broken lines) shown in arbitrary units and the distance from the center of an isolated nucleus, respectively. Compared with a relaxed nucleus (a), brightness at both sides of the contracted nucleus (b) showed sharper profiles (open and filled arrows). Furthermore, dark and bright areas appeared just inside both edges (filled and open arrowheads), and brightness inside the nucleus showed a rough and disordered profile. Bars = 10 μm.

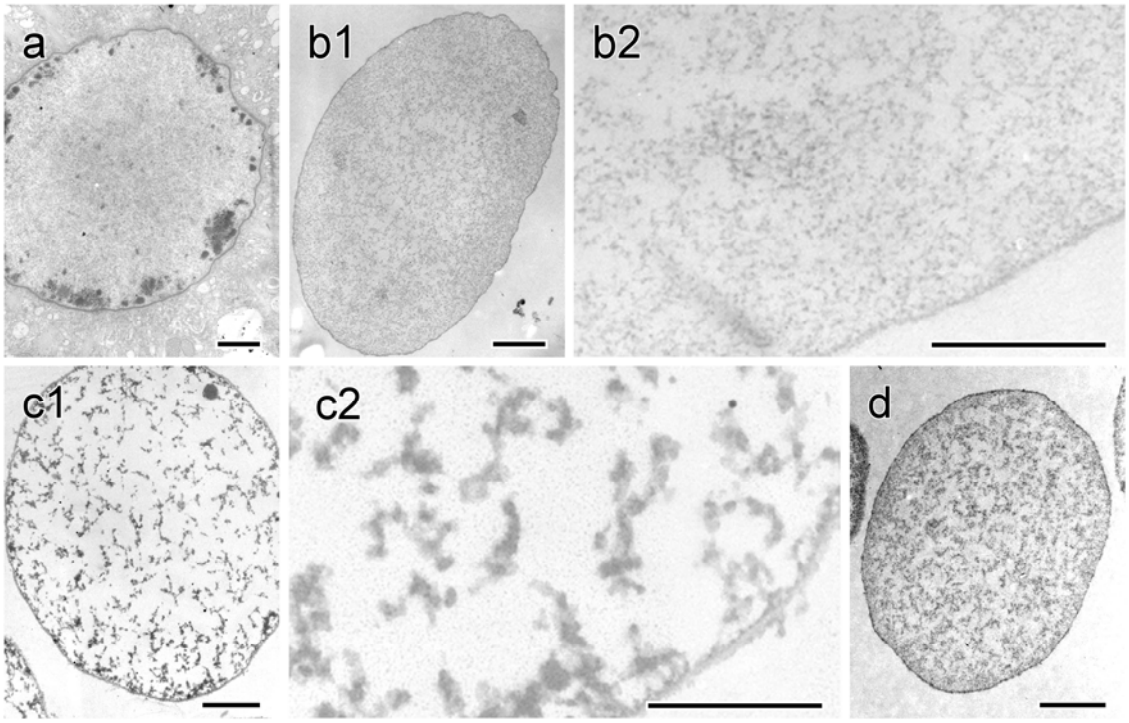

Fig. 7. Electron micrographs showing ultrastructural changes of isolated nuclei during Ca^{2+}-dependent contraction and expansion. (a) After fixation of a nucleus in a living cell, electron dense nucleolar material was located just beneath the nuclear membrane, and a meshwork of thin filaments was evenly distributed inside the nucleus. (b) In an isolated and detergent-extracted nucleus, the nucleolar material disappeared during isolation procedures, but the meshwork structure (b2, shown in higher magnification) was well preserved even after isolation. (c) On addition of Ca^{2+} (2 mM free Ca^{2+}), thin filaments became aggregated to form thicker filaments. c1 and c2 are taken in different magnifications. (d) The thicker filaments were disintegrated and became loose upon subsequent addition of EGTA (3 mM). Bars represent 2 μm, except for enlarged micrographs b2 and c2 (1 μm).